Computational Journal of Mathematical and Statistical Sciences
4(2), 379–406
DOI:10.21608/cjmss.2025.346849.1095
https://cjmss.journals.ekb.eg/

Research article

Type II half-logistic Ailamujia distribution with numerical illustrations to medical data

Ibrahim E. Ragab[1,*], **Mohammed Elgarhy**[2]

[1] Department of Basic Sciences, Egyptian Institute of Alexandria Academy for Management and Accounting, EIA, 21513 Alexandria, Egypt; ibrahim.ragab@eia.edu.eg

[2] Department of Basic Sciences, Higher Institute for Administrative Sciences, Belbeis, 44621 AlSharkia, Egypt; dr.moelgarhy@gmail.com

* **Correspondence:** ibrahim.ragab@eia.edu.eg

Abstract: In this article, we introduce a new two-parameter distribution called the type II half-logistic Ailamujia distribution, which is constructed from the type II half-logistic-G family and Ailamujia distribution. The probability density function exhibits decreasing, unimodal, and right-skewed shapes, whereas the hazard rate function shows decreasing, J-shaped, increasing, and inverted trends. Several statistical characteristics for the type II half-logistic Ailamujia distribution were computed, such as moments, moment-generating function, probability weighted moment, incomplete moments, conditional moments, mean deviation, Lorenz and Bonferroni curves, mean residual life, mean inactivity time and order statistics. Several uncertainty measures were computed and discussed theoretically and numerically. In addition, the maximum likelihood estimation method is used for the type II half-logistic Ailamujia distribution to estimate its two parameters. A thorough numerical analysis was carried out to evaluate the maximum likelihood strategy of the estimation's efficacy. The practicality and significance of a recently created model can be established by examining two real datasets. The type II half-logistic Ailamujia distribution is compared with numerous well-known statistical distributions such as Ailamujia, exponentiated Ailamujia, exponentiated exponential, gamma, and generalized Lindley models by utilizing different metrics. The numerical findings revealed that the type II half-logistic Ailamujia model suited the data better than the other competing models.

Keywords: Ailamujia distribution; Type II half-logistic family; Entropy measures; Monte-Carlo simulation; Order statistics; Mean residual life.

Mathematics Subject Classification: 60E05, 62E10, 62F10.

Received: 23 December 2024; Revised: 19 April 2025; Accepted: 26 April 2025; Online: 28 April 2025.

1. Introduction

This novel distribution provides additional flexibility in simulating failure rates, making it suitable for a wide range of practical applications. Extending current distributions allows researchers to create more precise models that closely match the available data. New probability distributions were developed and tested to advance statistical theory and methodology, ultimately improving our ability to make data-driven judgments. Applying these innovative distributions to real-world datasets illustrates their worth and importance in various industries, including reliability engineering, banking, and insurance. In essence, continuous innovation in probability theory propels the development of statistical modeling and analysis. [1] established the *Ailamujia distribution* (AD) for evaluating real−life data. This distribution is useful for anticipating maintenance time because it is flexible and includes distribution delays. Let W be a random variable that indicates the product's lifetime according to AD. AD can be identified by its *cumulative distribution function* (CDF) [takes $\psi = 2\theta$]

$$G(w;\psi) = 1 - (1 + \psi w)\, \mathrm{e}^{-\psi w}, \quad w > 0, \psi > 0. \tag{1.1}$$

The appropriate *probability density function* (pdf) is presented as follows:

$$g(w;\psi) = \psi^2 w e^{-\psi w}; \quad w > 0, \psi > 0. \tag{1.2}$$

Several authors have made great contributions to the study of AD. Pan et al. [2] examined interval estimation and hypothesis testing using a small sample size. [3] utilized conjugate prior, Jeffrey's prior, and non-informative prior distributions to estimate Bayesian models with type II censoring. Yu et al. [4] employed AD to examine the incidence and distribution of combat injuries during a campaign. Jan et al. [5] introduced and investigated a weighted version of AD, which outperformed the standard model. Jamal et al. [6] recently presented the *power Ailamujia* (PA) distribution, which is an extension of AD with a power transformer and a reparameterization. The idea is straightforward: adding a shape parameter increases the flexibility of the distribution. In recent years, many authors have extended AD, such as: exponentiated AD by [7], alpha power AD by [8], Marshall-Olkin power AD by [9], power-Lindley AD by [10] and weighted inverse AD by [11].

There has been a recent surge in interest in the development of new generators for univariate continuous distributions by introducing one or more additional shape parameter(s) into the base model. The inclusion of these parameter(s) has proven to be effective in examining the tail characteristics and enhancing the goodness-of-fit of the proposed generator group. These distributions were formulated by incorporating additional parameters into a baseline distribution to establish a novel set of skewed distributions that offer greater analytical versatility. Consequently, numerous categories have emerged in the statistical literature. Among the prominent generators are logistic-X-G proposed by [12], gamma-G developed by [13], sine-G studied by [14], Kumaraswamy-G introduced by [15], new heavy-tailed-G discussed by [16], McDonald-G presented by [17], odd inverse Weibull-G family by [18], odd hyperbolic cosine-G introduced by [19], Zografos-Balakrishnan-G proposed by [20], arcsine exponentiated-X G suggested by [21], truncated Muth-G proposed by [22], and odd inverse power generalized Weibull-G proposed by [23]. Hassan et al. [24] discussed the *type II half-logistic-G* (TIIHL-G) family. Define $G(w;\varsigma)$ as the CDF and $g(w;\varsigma)$ as the pdf of the baseline distribution, then the CDF and pdf for the TIIHL-G family respectively, are given by:

$$F(w;\varsigma) = \frac{2G^{\delta}(w;\varsigma)}{1 + G^{\delta}(w;\varsigma)}; \quad w \in \Re \tag{1.3}$$

and

$$g(w;\varsigma) = \frac{2\delta g(w;\varsigma)G^{\delta-1}(w;\varsigma)}{\left[1+G^{\delta}(w;\varsigma)\right]^2}; \quad w \in \Re, \tag{1.4}$$

where δ is a positive shape parameter.

The primary aim of this paper is to introduce and analyze the statistical properties of a novel two-parameter model referred to as the *type II half-logistic Ailamujia* (TIIHLA) distribution. The investigation of this model was motivated by the following considerations:

1. The TIIHLA distribution displays an extensive variety of graphical representations for the pdf and the *hazard rate function* (hrf).
2. Various statistical properties of the TIIHLA distribution are explored, including moments, moment-generating function, probability weighted moment, incomplete moments, conditional moments, mean deviation, Lorenz and Bonferroni curves, mean residual life, mean inactivity time, and order statistics.
3. The *maximum likelihood* (ML) estimation technique is utilized to estimate the two parameters of the TIIHLA distribution. A comprehensive numerical procedure was performed to determine whether the ML estimation technique was effective.
4. To outperform competing models, we compared TIIHLA distribution against several alternative models such as Ailamujia, exponentiated Ailamujia, exponentiated exponential, gamma, and generalized Lindley models using two real-world datasets. The TIIHLA distribution consistently demonstrated superior performance.

The remainder of this paper is organized as follows: Section 2 establishes the framework for the TIIHLA distribution. Section 3 delineates significant mixture representations of its pdf and CDF. Section 4 analyzes various statistical properties associated with the distribution. Sections 5 and 6 explore differing measurements of entropy and the order statistics, respectively. Sections 7 and 8 focus on parameters estimation and the results of simulation studies. Finally, Section 9 presents insights derived from real data, while Section 10 offers concluding remarks.

2. Model Formulation

This section explores the main distribution functions of the TIIHLA model utilizing both mathematical and visual methods. As stated in the introduction, the CDF of the TIIHLA distribution is produced by combining Equations (1.1) and (1.3), which can be expressed as follows:

$$F(w;\psi,\delta) = \frac{2\left[1-(1+\psi\, w)\ \mathrm{e}^{-\psi w}\right]^{\delta}}{1+\left[1-(1+\psi\, w)\ \mathrm{e}^{-\psi w}\right]^{\delta}} \quad ; \quad w>0,\ \psi,\delta>0\ . \tag{2.1}$$

The relevant pdf is derived by substituting Equation (1.2) into Equation (1.4):

$$f(w;\psi,\delta) = \frac{2\,\delta\,\psi^2\, w\,\mathrm{e}^{-\psi w}\left[1-(1+\psi\, w)\ \mathrm{e}^{-\psi w}\right]^{\delta-1}}{\left[1+\left\{1-(1+\psi\, w)\ \mathrm{e}^{-\psi w}\right\}^{\delta}\right]^2}. \tag{2.2}$$

The *survival or reliability function* (SF) determines the probability of an item surviving during a given time range. In engineering, the phrase "reliability" is usually used, while the term "survival" relates to

human mortality. The TIIHLA distribution's SF is described as:

$$S(w;\psi,\delta) = \frac{1-\left[1-(1+\psi\, w)\ \mathrm{e}^{-\psi w}\right]^{\delta}}{1+\left[1-(1+\psi\, w)\ \mathrm{e}^{-\psi w}\right]^{\delta}}. \tag{2.3}$$

The hrf is an essential idea in survival analysis, and is commonly used in medical research to determine the time until an event of interest occurs. This serves to evaluate the probability of an event occurring at specific times, assuming that it has not yet occurred. For the proposed model, the hrf is given by:

$$h(w;\psi,\delta) = \frac{2\,\delta\,\psi^2\, w\,\mathrm{e}^{-\psi w}\left(1-(1+\psi\, w)\,\mathrm{e}^{-\psi w}\right)^{\delta-1}}{1-\left[1-(1+\psi\, w)\,\mathrm{e}^{-\psi w}\right]^{2\delta}}. \tag{2.4}$$

Figures 1-3 depict the pdf and hrf of the proposed model. As shown in Figures 1-3, the pdf exhibits a decreasing, unimodal and right-skewed form, whereas the hrf demonstrates decreasing, J-shaped, increasing and inverted trends. This variability underscores the model's adaptability in representing a wide range of distributional characteristics and hazard-rate profiles.

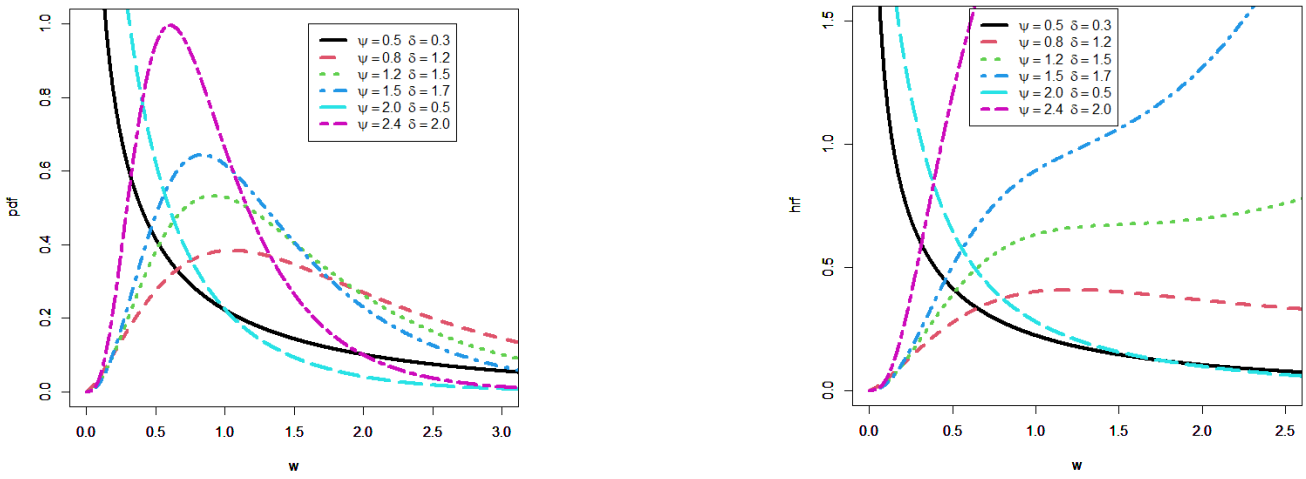

Figure 1. Plots of the pdf and hrf across a range of parameter values.

3. Mixture Representation

This section presents series representations for the pdf and CDF derived from the generalized binomial expansion. We begin by recalling that for any real number $a > 0$ and $|\varepsilon| < 1$, the generalized binomial series is defined as follows:

$$(1+\varepsilon)^{-a} = \sum_{n=0}^{\infty}(-1)^n \binom{a+n-1}{n} \varepsilon^n, \tag{3.1}$$

by employing this extension, Equation (2.2) can be reformulated as:

$$f(w;\psi,\delta) = \sum_{i,j=0}^{\infty} 2\,(-1)^{i+j}\,(i+1)\binom{(i+1)\delta-1}{j}\,\delta\,\psi^2\, w\,(1+\psi\, w)^j\ \mathrm{e}^{-\psi\,(j+1)\,w}. \tag{3.2}$$

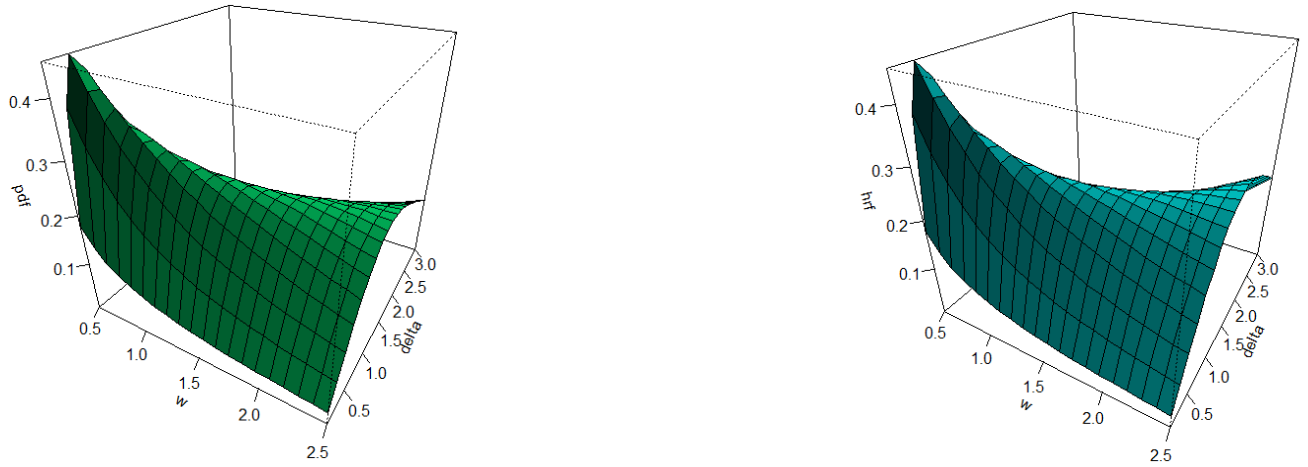

Figure 2. 3D Plots of the pdf and hrf at $\psi = 0.5$.

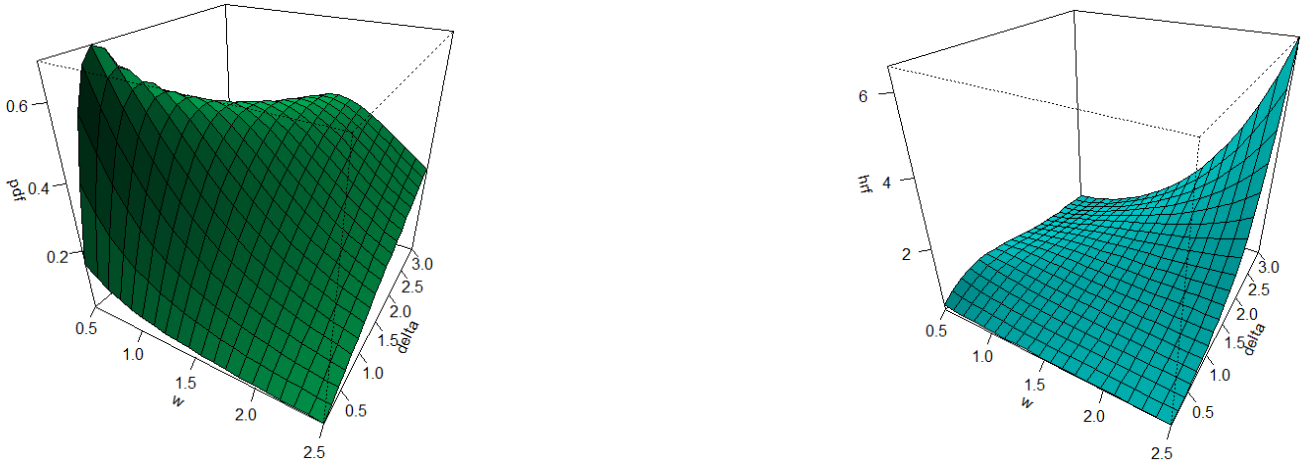

Figure 3. 3D Plots of the pdf and hrf across at $\psi = 1.2$.

Furthermore, using the normal power series expansion.

$$(1+b)^z = \sum_{h=0}^{\infty} \binom{z}{h} b^h; \quad \text{for } |b| < 1 \text{ and } z \text{ is a positive real non-integer} \tag{3.3}$$

the pdf of the TIIHLA distribution can be expressed as:

$$f(w;\psi,\delta) = \sum_{i,j,k=0}^{\infty} \pi_{i,j,k}\, w^{k+1}\ \mathrm{e}^{-\psi\,(j+1)\,w}\ , \tag{3.4}$$

where the coefficient $\pi_{i,j,k}$ is defined as:

$$\pi_{i,j,k} = 2\,(-1)^{i+j}\,(i+1) \binom{(i+1)\delta - 1}{j} \binom{j}{k} \delta\, \psi^{k+2}\ .$$

We now derive an analytical expression for $[F(w;\psi,\delta)]^m$, where m is an integer, using Equation (3.1),

yields:

$$[F(w;\psi,\delta)]^m = \sum_{v=0}^{\infty} 2^m(-1)^v \binom{m+v-1}{v} \left[1-(1+\psi\, w)\ \mathrm{e}^{-\psi\ w}\right]^{\delta(m+v)}$$

Next, the term $\left[1-(1+\psi\, w)\ \mathrm{e}^{-\psi\ w}\right]^{\delta(m+v)}$ is rewritten using the generalized binomial expansion as:

$$\left[1-(1+\psi\, w)\ \mathrm{e}^{-\psi\ w}\right]^{\delta(m+v)} = \sum_{b=0}^{\infty}(-1)^b \binom{\delta(m+v)}{b} (1+\psi\, w)^b\ \mathrm{e}^{-b\ \psi\ w}$$

Subsequently, by employing Formula (3.3) for the expansion of $(1+\psi\, w)^b$, the expression of $[F(w;\psi,\delta)]^m$can be reformulated as:

$$[F(w;\psi,\delta)]^m = \sum_{v,b,l=0}^{\infty} \eta_{v,b,l}\, w^l\, \mathrm{e}^{-b\ \psi\ w}, \tag{3.5}$$

with the coefficient $\eta_{v,b,l}$ is defined by:

$$\eta_{v,b,l} = 2^m\,(-1)^{v+b} \binom{m+v-1}{v} \binom{\delta(m+v)}{b} \binom{b}{l} \psi^l\ .$$

Series representations (3.4) and (3.5) facilitate the determination of the statistical properties for the proposed model.

4. Statistical Properties

This section thoroughly explores the key statistical properties of the TIIHLA distribution. In particular, we derive and discuss its moments, moment-generating function, probability-weighted moment, incomplete moments, and conditional moments. Additionally, we look at the mean deviation, Lorenz and Bonferroni curves, mean residual life, and mean inactivity time. These properties provide a detailed insight into the distribution's behavior and its potential applications in various analytical contexts.

4.1. Moments

Statistical moments are numerical metrics that are used to describe the shape and dispersion of a distribution. They contribute to the summary of the data distribution and provide insights into its properties. The first four statistical moments are; the first moment [mean: $\mu = \mu_1^{'}$] is the average of all data values and represents the distribution's center. The second moment [variance: $\sigma_w^2 = \mu_2^{'} - (\mu_1^{'})^2$] indicates the spread of the data around the mean. The third moment [skewness: $\gamma_1 = \left[\mu_3^{'} - 3\,\mu_1^{'}\,\mu_2^{'} + 2\,(\mu_1^{'})^3\right] \Big/ \sigma_w^3$] denotes asymmetry in the distribution; negative skew suggests a longer left tail, while positive skew indicates a longer right tail. The fourth moment [kurtosis: $\gamma_2 = \left[\mu_4^{'} - 4\,\mu_1^{'}\,\mu_3^{'} + 6\,(\mu_1^{'})^2\,\mu_2 - 3(\mu_1^{'})^4\right] \Big/ \sigma_w^4$] determines whether a distribution is highly peaked or spread out; a high kurtosis suggests a sharp peak, while a low kurtosis indicates a more spread out distribution. Moreover, the *coefficient of variation* [$CV = \sigma_w/\mu$] assesses the spread of data points in comparison with the mean. In general, ordinary moments are significant in statistical analysis because they provide crucial insight into data distribution, resulting in more accurate results. The r^{th} moment about the origin of the TIIHLA distribution is

calculated by utilizing the pdf (3.4) as follows:

$$\mu_r^{'}(w) = E(w^r) = \int_0^{\infty} w^r \, f(w;\psi,\delta) \, d\, w$$

$$\mu_r^{'}(w) = \sum_{i,j,k=0}^{\infty} \pi_{i,j,k} \int_0^{\infty} w^{r+k+1} \, \mathrm{e}^{-\psi\,(j+1)\,w} \, d\, w$$

$$= \sum_{i,j,k=0}^{\infty} \pi_{i,j,k} \, \frac{\Gamma(r+k+2)}{[(j+1)\,\psi]^{r+k+2}} \, ; \quad r = 1, 2, \ \ldots \tag{4.1}$$

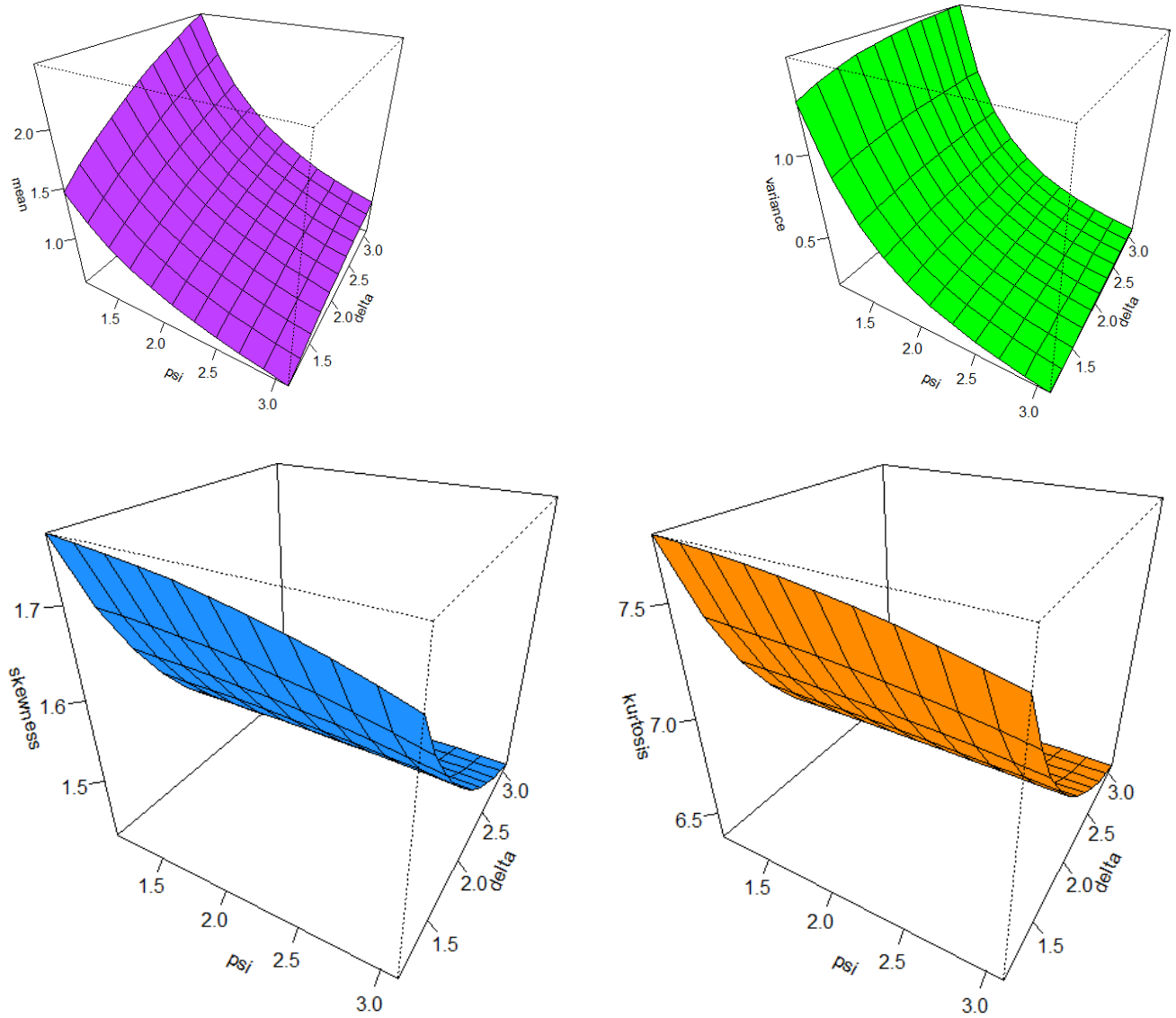

Figure 4. 3D Plots of the mean, variance, skewness and kurtosis for the TIIHLA model.

Table 1 illustrates the numerical results for the first four moments, variance, skewness, kurtosis, and CV for the proposed model at different levels of parameters ψ and δ. As the values of these parameters

increase, consequently increase the first four moments and variance, whereas the skewness, kurtosis, and CV decrease. Figure 4 displays visual confirmation of these findings.

Table 1. A numerical representation of the first four moments, σ_w^2 , γ_1 , γ_2 and the CV

ψ ↑	δ ↑	μ_1 ↑	μ_2 ↑	μ_3 ↑	μ_4 ↑	σ_w^2 ↑	γ_1 ↓	γ_2 ↓	CV ↓
0.5	0.5	1.87775	8.14712	55.9948	519.696	4.62116	2.34967	10.9659	1.144820
	1.0	3.04665	15.2737	109.738	1032.62	5.99158	1.82026	8.00707	0.803430
	1.5	3.85630	21.4303	160.557	1535.06	6.55925	1.62669	7.13877	0.664135
	2.0	4.47062	26.8315	208.520	2025.60	6.84510	1.52789	6.74362	0.585225
	3.0	5.37536	35.9971	296.922	2970.48	7.10262	1.42992	6.38790	0.495795
	5.0	6.55489	50.2079	450.459	4728.10	7.24129	1.35587	6.14920	0.410528
1	0.5	0.93888	2.03678	6.99935	32.48100	1.15529	2.34967	10.9659	1.14482
	1.0	1.52333	3.81842	13.71720	64.53890	1.49790	1.82026	8.00707	0.80343
	1.5	1.92815	5.35757	20.06960	95.94130	1.63981	1.62669	7.13877	0.66414
	2.0	2.23531	6.70788	26.06500	126.6000	1.71128	1.52789	6.74362	0.58523
	3.0	2.68768	8.99927	37.11530	185.65500	1.77566	1.42992	6.38790	0.49580
	5.0	3.27745	12.552	56.3074	295.50700	1.81032	1.35587	6.1492	0.410528
2	0.5	0.46944	0.50920	0.87492	2.030060	0.28882	2.34967	10.9659	1.14482
	1.0	0.76166	0.95460	1.71466	4.033680	0.37447	1.82026	8.00707	0.80343
	1.5	0.96408	1.33939	2.50870	5.996330	0.40995	1.62669	7.13877	0.66414
	2.0	1.11765	1.67697	3.25812	7.912510	0.42782	1.52789	6.74362	0.58523
	3.0	1.34384	2.24982	4.63941	11.60340	0.44391	1.42992	6.38790	0.49580
	5.0	1.63872	3.13799	7.03843	18.46920	0.45258	1.35587	6.14920	0.41053
2.5	0.5	0.375551	0.325885	0.447959	0.831513	0.184846	2.34967	10.9659	1.144820
	1.0	0.609330	0.610947	0.877904	1.652200	0.239663	1.82026	8.00707	0.803430
	1.5	0.771260	0.857212	1.284460	2.456100	0.262370	1.62669	7.13877	0.664135
	2.0	0.894123	1.073260	1.668160	3.240960	0.273804	1.52789	6.74362	0.585225
	3.0	1.075070	1.439880	2.375380	4.752770	0.284105	1.42992	6.38790	0.495795
	5.0	1.310980	2.008320	3.603680	7.564970	0.289651	1.35587	6.14920	0.410528
3	0.5	0.312959	0.226309	0.259235	0.401000	0.128366	2.349670	10.965900	1.144820
	1.0	0.507775	0.424268	0.508046	0.796777	0.166433	1.820260	8.007070	0.803430
	1.5	0.642716	0.595286	0.743320	1.184460	0.182201	1.626690	7.138770	0.664135
	2.0	0.745103	0.745320	0.965370	1.562970	0.190142	1.527890	6.743620	0.585225
	3.0	0.895893	0.999919	1.374640	2.292040	0.197295	1.429920	6.387900	0.495795
	5.0	1.092480	1.394660	2.085460	3.648230	0.201147	1.355870	6.149200	0.410528
3.5	0.5	0.268250	0.166268	0.163250	0.216450	0.094309	2.349670	10.965900	1.144820
	1.0	0.435236	0.311707	0.319936	0.430080	0.122277	1.820260	8.007070	0.803430
	1.5	0.550900	0.437353	0.468096	0.639342	0.133862	1.626690	7.138770	0.664135
	2.0	0.638659	0.547582	0.607930	0.843650	0.139696	1.527890	6.743620	0.585225
	3.0	0.767908	0.734634	0.865663	1.237180	0.144951	1.429920	6.387900	0.495795
	5.0	0.936413	1.024650	1.313290	1.969220	0.147781	1.355870	6.149200	0.410528

4.2. Moment-generating function

The *moment-generating function* (MGF) is a fundamental tool in probability theory. It enables the efficient calculation of a random variable's moments and simplifies the analysis of sums of random variables through the convolution property. Furthermore, the uniqueness property of the MGF ensures that if two random variables possess identical MGFs (within a neighborhood of the origin where the MGF converges), their probability distributions are necessarily equivalent. The MGF of the TIIHLA distribution is derived using the pdf (3.4) as follows:

$$m(w) = \int_0^\infty e^{t\,w} f(w;\psi,\delta)\; d\,w$$

$$= \sum_{i,j,k=0}^{\infty} \pi_{i,j,k} \int_0^\infty w^{k+1}\, e^{[t-\psi\,(j+1)]\,w}\, d\,w$$

$$= \sum_{i,j,k=0}^{\infty} \pi_{i,j,k}\, \frac{\Gamma(k+2)}{[(j+1)\,\psi - t]^{k+2}} \;\; ; \;\; t < \;(j+1)\,\psi \;\; , \tag{4.2}$$

4.3. Probability weighted moment

The *probability weighted moment* (PWM) approach is commonly used for estimating parameters in distributions that lack a straightforward inverse form. First introduced in [25], this method has gained significant recognition in hydrological studies for estimating purposes. The PWM of the TIIHLA distribution is obtained as:

$$\rho(w) = E\left[w^r F^m(w;\psi,\delta)\right] = \int_0^\infty w^r\; \left[F(w;\psi,\delta)\right]^m f(w;\psi,\delta)\; d\,w \tag{4.3}$$

By substituting Equations (3.4) and (3.5) into Equation (4.3), we obtain:

$$\rho(w) = \sum_{i,j,k=0}^{\infty} \sum_{v,b,l=0}^{\infty} \pi_{i,j,k}\, \eta_{v,b,l} \int_0^\infty w^{r+k+l+1} e^{-\psi\,(j+b\,+1)\;w} d\,w$$

$$= \sum_{i,j,k=0}^{\infty} \sum_{v,b,l=0}^{\infty} \pi_{i,j,k}\, \eta_{v,b,l}\, \frac{\Gamma(r+k+l+2)}{[\,(j+b\;+1)\,\psi]^{r+k+l+2}} \;\; .$$

4.4. Incomplete moments

Incomplete moments (IMs) provide a framework for characterizing a distribution by concentrating on a specific sub-range of values rather than its entire domain. This targeted approach, which focuses on values that exceed or fall below a designated threshold, is particularly effective for analyzing tail behavior and emphasizing critical portions of the distribution. In the field of economics, IMs are indispensable for quantifying inequality. For example, income quintiles facilitate the assessment of disparities among different segments of the population. Furthermore, the *Lorenz curve* (Lz), which is derived from IMs, offers a visual representation of the distribution of income or wealth, while the

Bonferroni index (Bo) furnishes an additional quantitative measure of inequality. The s^{th} IMs of the TIIHLA distribution can be expressed as follows:

$$\begin{aligned}\kappa_s(w) = E\left(w^s \mid W < t\right) &= \int_0^t w^s f(w;\psi,\delta)\, d\, w \\ &= \sum_{i,j,k=0}^{\infty} \pi_{i,j,k} \int_0^t w^{s+k+1}\, \mathrm{e}^{-\psi\,(j+1)\,w}\, d\, w \\ &= \sum_{i,j,k=0}^{\infty} \pi_{i,j,k}\, \frac{\gamma\left[s+k+2,\ (j+1)\,\psi\, t\right]}{\left[(j+1)\,\psi\right]^{k+s+2}}\ ,\end{aligned} \tag{4.4}$$

where, $\gamma(\tau,\varsigma) = \int_0^{\varsigma} y^{\tau-1}\ e^{-y}\, dy$ indicates the lower incomplete gamma function. Substituting $s = 1$ into Equation (4.4), yields the first IM of the TIIHLA distribution as:

$$\kappa_1(w) = \sum_{i,j,k=0}^{\infty} \pi_{i,j,k}\, \frac{\gamma\left[k+3,\ (j+1)\,\psi\, t\right]}{\left[(j+1)\,\psi\right]^{k+3}}\ . \tag{4.5}$$

To evaluate the Lz and the Bo, we employ the following equations: $Lz = \kappa_1(w)/\mu$ and $Bo = \kappa_1(w)/p \times \mu$, where $q = F^{-1}(p)$ denotes the quantile corresponding to the probability p. Furthermore, Equation (4.5) is employed to derive the mean deviation about μ or median (M_d), which are expressed as follows:

$$\varphi_1(w) = E\left[\mid W - \mu \mid\right] = 2\,\mu\, F(\mu) - 2\,\kappa_1(\mu)\ ,$$

or

$$\varphi_2(w) = E\left[\mid W - M_d \mid\right] = \mu - 2\,\kappa_1(M_d)\ ,$$

where, $F(\mu)$ is obtained from Equation (2.1).

4.5. Conditional moments

Conditional moments (CMs) are crucial in many statistical techniques, such as regression and hypothesis testing, for showing the relationship between variables and their responses in various contexts. For instance, in regression analysis, these moments can predict the value of the dependent variable using particular independent variable values, offering valuable insights into variable behavior across different conditions and enhancing forecasting accuracy. The CMs of the TIIHLA distribution can be represented as:

$$E\left(w^s \mid W > t\right) = \frac{\eta_s(t)}{1 - F(w;\psi,\delta)}\ ,$$

the term $\eta_s(t)$ can be derived as follows:

$$\begin{aligned}\eta_s(t) &= \int_t^{\infty} w^s\, f(w;\psi,\delta)\, d\, w \\ &= \sum_{i,j,k=0}^{\infty} \pi_{i,j,k} \int_t^{\infty} w^{s+k+1}\, \mathrm{e}^{-\psi\,(j+1)\,w}\, d\, w \\ &= \sum_{i,j,k=0}^{\infty} \pi_{i,j,k}\, \frac{\Gamma\left[s+k+2,\ (j+1)\,\psi\, t\right]}{\left[(j+1)\,\psi\right]^{k+s+2}}\ ,\end{aligned} \tag{4.6}$$

such that, $\Gamma(\tau,\varsigma) = \int_{\varsigma}^{\infty} y^{\tau-1}\ e^{-y}\ dy$ denotes the upper incomplete gamma function.

4.6. Mean residual life and mean inactivity time

In survival analysis and reliability theory, the *mean residual life* (MRL) is employed to predict the remaining lifetime of an individual or system that has survived up to a specific time point. This function is widely utilized in healthcare, actuarial science, and the social sciences to analyze and forecast future survival and mortality outcomes. The MRL for the TIIHLA distribution is determined as:

$$MRL(t) = E\left(W - t \mid W > t\right) = \frac{\eta_1(t)}{1 - F(t;\psi,\delta)} - t,$$

utilizing Equation (4.5) for computing the first CM:

$$\eta_1(t) = \sum_{i,j,k=0}^{\infty} \pi_{i,j,k} \, \frac{\Gamma\left[k+3, (1+j)\,\psi\, t\right]}{\left[(j+1)\psi\right]^{k+3}},$$

using Equation (2.1), the MRL is described as:

$$MRL(t) = -t + \frac{1 + \left[1 - (1+\psi\, t)\, \mathrm{e}^{-\psi t}\right]^{\delta}}{1 - \left[1 - (1+\psi\, t)\, \mathrm{e}^{-\psi t}\right]^{\delta}} \sum_{i,j,k=0}^{\infty} \pi_{i,j,k} \, \frac{\Gamma\left[k+3, (j+1)\,\psi\, t\right]}{\left[(j+1)\psi\right]^{k+3}}, \tag{4.7}$$

The *mean inactivity time* (MIT), also called mean past lifetime or mean waiting time, is a key reliability metric in survival analysis, risk theory and actuarial studies. It provides insight into the average duration of inactivity for a system or component. The MIT for the TIIHLA distribution is derived as:

$$MIT(t) = E\left(W \mid W < t\right) = t - \frac{\kappa_1(t)}{F(t;\psi,\delta)}; \quad t > 0,$$

by applying Equation (4.5) in conjunction with Equation (2.1), we obtain:

$$MIT(t) = t - \frac{1 + \left[1 - (1+\psi\, t)\, \mathrm{e}^{-\psi t}\right]^{\delta}}{2\left[1 - (1+\psi\, t)\, \mathrm{e}^{-\psi t}\right]^{\delta}} \sum_{i,j,k=0}^{\infty} \pi_{i,j,k} \, \frac{\gamma\left[k+3, (j+1)\,\psi\, t\right]}{\left[(j+1)\,\psi\right]^{k+3}}. \tag{4.8}$$

Table 2 presents the MRL and MIT of the TIIHLA distribution for various parameter levels. The results indicate that as the parameter values increase, the MRL increases, while the MIT decreases.
Figure 5 shows how MRL and MIT change in response to variations in distribution parameters. The left panel shows a significant decline in MRL as parameter values increase, while the right panel shows a considerable increase in MIT under the same conditions.

5. Entropy Measures

In [26], entropy was first introduced in physics as a measure of the energy within a system that cannot be used to perform work. Early studies in statistical mechanics and gas dynamics later connected this idea to the behavior of atoms. Over time, entropy has become fundamental in multi-particle physics, particularly in the analysis of non-equilibrium processes as guided by the second law of thermodynamics and the principle of maximum entropy generation. In addition, [27] incorporated Shannon entropy into his theories of information and communication, a concept that continues to be vital in modern artificial intelligence and collaborative methodologies.

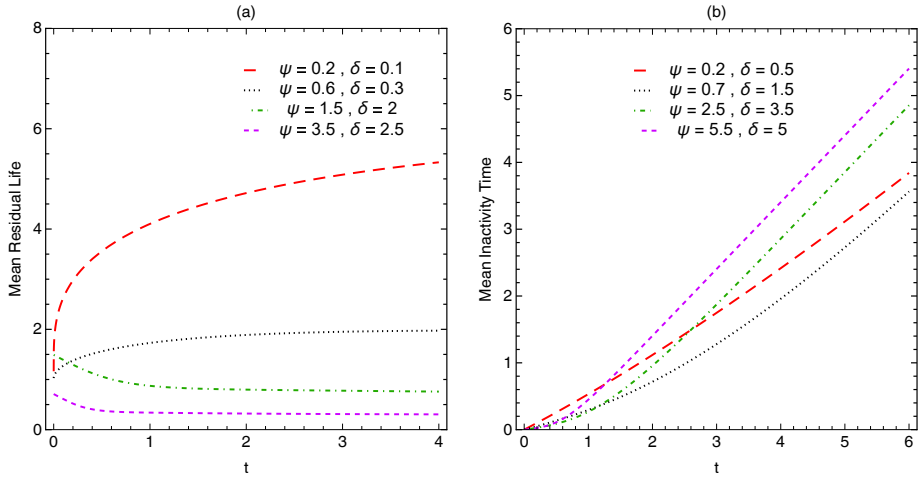

Figure 5. Plots of the MRL (left) and MIT (right) for the TIIHLA distribution.

Table 2. The MRL and MIT of the TIIHLA distribution

$\psi \uparrow$	$\delta \uparrow$	$MRL \uparrow$	$MIT \downarrow$	$\psi \uparrow$	$\delta \uparrow$	$MRL \uparrow$	$MIT \downarrow$
1	0.5	1.18019	1.39452	2.5	0.5	0.46194	1.64620
	1.0	1.19337	1.04743		1.0	0.46197	1.42970
	1.5	1.21493	0.83386		1.5	0.46203	1.28272
	2.0	1.24425	0.69001		2.0	0.46210	1.17333
	3.0	1.32300	0.51038		3.0	0.46232	1.01634
	5.0	1.53505	0.33564		5.0	0.46302	0.82103
1.5	0.5	0.78981	1.50115	3	0.5	0.37931	1.69612
	1.0	0.79143	1.20525		1.0	0.37931	1.50875
	1.5	0.79410	1.01277		1.5	0.37932	1.38038
	2.0	0.79783	0.87539		2.0	0.37933	1.28401
	3.0	0.80836	0.68951		3.0	0.37936	1.14410
	5.0	0.84083	0.48256		5.0	0.37946	0.96637
2	0.5	0.58605	1.58263	3.5	0.5	0.32085	1.73551
	1.0	0.58628	1.33031		1.0	0.32085	1.57169
	1.5	0.58665	1.16165		1.5	0.32085	1.45887
	2.0	0.58717	1.03796		2.0	0.32085	1.37375
	3.0	0.58866	0.86401		3.0	0.32085	1.24934
	5.0	0.59338	0.65553		5.0	0.32087	1.08940

In probability theory, entropy quantifies the inherent unpredictability of a random variable. A higher entropy value signifies a greater level of uncertainty in possible outcomes. Widely used in data analysis and computer science, entropy serves as a quantitative measure for assessing uncertainty within datasets and systems. Below is a concise overview of the different types of entropy.

1. *Rényi entropy* (RE) is a key concept for estimating fractal dimensions. It is applied in ecology and statistics as a diversity index, as well as in quantum information theory to quantify uncertainty (see [26]). The RE of a random variable W following the TIIHLA distribution can be computed as:

$$RE(\vartheta) = \frac{1}{1-\vartheta} \log\left[\int_0^\infty f^\vartheta(w;\psi,\delta)\, dw\right] ; \vartheta > 0,\ \vartheta \neq 1\,,$$

the term $f^\vartheta(w;\psi,\delta)$ can be stated as follows:

$$f^\vartheta(w;\psi,\delta) = \sum_{i,j,k=0}^{\infty} \tau_{i,j,k}\ w^{k+\vartheta}\ e^{-\psi\,(j+\vartheta)\,w}$$

where,

$$\tau_{i,j,k} = (2\,\delta)^\vartheta\ \psi^{k+2\vartheta}\ (-1)^{i+j} \binom{j}{k} \binom{2\,\vartheta+i-1}{i} \binom{\delta(\vartheta+i)-\vartheta-1}{j}\,.$$

The integral of $f^\vartheta(w;\psi,\delta)$ can be derived as:

$$\int_0^\infty f^\vartheta(w;\psi,\delta)\, d\,w = \sum_{i,j,k=0}^{\infty} \tau_{i,j,k} \int_0^\infty w^{k+\vartheta}\ e^{-\psi\,(j+\vartheta)\ w}\, d\,w$$

$$= \sum_{i,j,k=0}^{\infty} \tau_{i,j,k} \frac{\Gamma\,(k+\vartheta+1)}{[(j+\vartheta)\ \psi]^{k+\vartheta+1}}\ .$$

Thus, the RE of the TIIHLA distribution is given by:

$$RE(\vartheta) = \frac{1}{1-\vartheta} \log\left[\sum_{i,j,k=0}^{\infty} \tau_{i,j,k} \frac{\Gamma\,(k+\vartheta+1)}{[(j+\vartheta)\ \psi]^{k+\vartheta+1}}\right] ; \vartheta > 0,\ \vartheta \neq 1\ . \tag{5.1}$$

1. *Tsallis entropy* (TE) has found widespread application across diverse fields, including physics, complex systems analysis, information theory, and economics [28]. Its utility stems from its capacity to characterize systems exhibiting long-range interactions or non-extensive behaviors, notably non-equilibrium systems and phase transitions. Serving as a valuable instrument in statistical mechanics, TE offers a generalized framework surpassing traditional entropy measures for the analysis of intricate systems and phenomena. The TE entropy for the TIIHLA distribution is defined as:

$$TE(\vartheta) = \frac{1}{\vartheta-1}\left[1 - \int_0^\infty f^\vartheta(w;\psi,\delta)\, dw\right] ; \vartheta > 0,\ \vartheta \neq 1$$

$$= \frac{1}{\vartheta-1}\left[1 - \sum_{i,j,k=0}^{\infty} \tau_{i,j,k} \frac{\Gamma\,(k+\vartheta+1)}{[(j+\vartheta)\ \psi]^{k+\vartheta+1}}\right]\ . \tag{5.2}$$

2. *Arimoto entropy* (AE) introduced by [29], is an extension of Shannon entropy that retains similar characteristics. This entropy measure quantifies the average uncertainty inherent in a stochastic variable, thereby reflecting its information content. The AE for the TIIHLA distribution is given by:

$$AE(\vartheta) = \frac{\vartheta}{1-\vartheta}\left[\left(\int_0^\infty f^\vartheta(w;\psi,\delta)\, dw\right)^{\frac{1}{\vartheta}} - 1\right] ; \vartheta > 0,\ \vartheta \neq 1$$

$$= \frac{\vartheta}{1-\vartheta}\left[\left(\sum_{i,j,k=0}^{\infty} \tau_{i,j,k} \frac{\Gamma(k+\vartheta+1)}{[(j+\vartheta)\,\psi]^{k+\vartheta+1}}\right)^{\frac{1}{\vartheta}} - 1\right]. \tag{5.3}$$

1. *Havrda-Charvát entropy* (HCE) is a parametric extension of Shannon entropy, developed by [30]. It has been applied in various domains, including deep learning for pulmonary end microscopy classification and training deep networks with limited datasets. The HCE for the TIIHLA distribution is given by:

$$HCE(\vartheta) = \frac{1}{2^{1-\vartheta}-1}\left[\int_0^\infty f^\vartheta(w;\psi,\delta)\, dw - 1\right] ;\ \vartheta > 0,\ \vartheta \neq 1$$

$$= \frac{1}{2^{1-\vartheta}-1}\left[\sum_{i,j,k=0}^{\infty} \tau_{i,j,k} \frac{\Gamma(k+\vartheta+1)}{[(j+\vartheta)\,\psi]^{k+\vartheta+1}} - 1\right]. \tag{5.4}$$

Tables 3 and 4 display the numerical estimates of the entropy measures for the TIIHLA distribution across a range of parameter values. This comprehensive presentation provides valuable insights into the variations of entropy under different conditions.

6. Order Statistics

Order statistics represent the values of a random sample when arranged in a specific order either ascending or descending. They capture essential statistical measures such as the minimum, maximum, percentiles, and quartiles, all of which provide deep insights into the data distribution. Suppose W_1, W_2, ..., W_n are independent random variables drawn from the TIIHLA distribution. When these variables are organized in ascending order as: $W_{(1)} < W_{(2)} < \ldots < W_{(n)}$. The pdf of the i^{th} order statistic is given by:

$$f_{i:n}(w;\psi,\delta) = \frac{f(w;\psi,\delta)}{Beta(i, n-i+1)} \sum_{j=0}^{n-i} (-1)^j \binom{n-i}{j} F^{i+j-1}(w;\psi,\delta). \tag{6.1}$$

Substituting the expressions from Equations (3.4) and (3.5) into Equation (6.1) and replacing m with $i+j-1$, produces:

$$f_{i:n}(w;\psi,\delta) = \frac{1}{Beta(i, n-i+1)} \sum_{j=0}^{n-i} \sum_{i,j,k,v,b,l=0}^{\infty} \eta *_{i,j,v,b,l}\ w^{k+l+1}\, e^{-\psi(j+b+1)\,w}, \tag{6.2}$$

Table 3. Numerical values of the entropy for the TIIHLA distribution ($\vartheta = 0.5$ or $\vartheta = 0.8$)

$\psi \uparrow$	$\delta \uparrow$	$\vartheta = 0.5$				$\vartheta = 0.8$			
		$RE(\vartheta) \uparrow$	$TE(\vartheta) \uparrow$	$AE(\vartheta) \uparrow$	$HCE(\vartheta) \uparrow$	$RE(\vartheta) \uparrow$	$TE(\vartheta) \uparrow$	$AE(\vartheta) \uparrow$	$HCE(\vartheta) \uparrow$
0.5	0.5	2.09616	3.70434	7.13487	4.47153	1.76560	2.11750	2.21952	2.84805
	1.0	2.35604	4.49587	9.54908	5.42700	2.12813	2.65274	2.80955	3.56794
	1.5	2.44678	4.79739	10.5511	5.79096	2.23840	2.82339	2.99989	3.79748
	2.0	2.49071	4.94835	11.0699	5.97318	2.28881	2.90267	3.08867	3.90411
	3.0	2.53132	5.09085	11.5700	6.14520	2.33356	2.97371	3.16842	3.99966
	5.0	2.54173	5.12785	11.7016	6.18987	2.36171	3.01872	3.21903	4.06020
1	0.5	1.40301	2.03358	3.06743	2.45474	1.07245	1.19615	1.22997	1.60882
	1.0	1.66289	2.59327	4.27454	3.13036	1.43498	1.66209	1.72613	2.23552
	1.5	1.75363	2.80648	4.77556	3.38772	1.54526	1.81066	1.88619	2.43535
	2.0	1.79757	2.91322	5.03494	3.51657	1.59567	1.87967	1.96084	2.52817
	3.0	1.83817	3.01399	5.28501	3.63820	1.64041	1.94152	2.02789	2.61135
	5.0	1.86485	3.08132	5.45496	3.71949	1.66856	1.98070	2.07046	2.66406
2	0.5	0.70987	0.85217	1.03372	1.02866	0.37930	0.39406	0.39787	0.53001
	1.0	0.96975	1.24794	1.63727	1.50639	0.74183	0.79969	0.81508	1.07559
	1.5	1.06049	1.39869	1.88778	1.68837	0.85211	0.92902	0.94967	1.24954
	2.0	1.10442	1.47417	2.01747	1.77948	0.90252	0.98910	1.01245	1.33035
	3.0	1.14502	1.54542	2.14251	1.86549	0.94727	1.04294	1.06883	1.40276
	5.0	1.17170	1.59304	2.22748	1.92297	0.97541	1.07706	1.10463	1.44865
2.5	0.5	0.48672	0.55106	0.62697	0.15616	0.15862	0.15925	0.21335	0.15616
	1.0	0.74660	0.90504	1.10982	0.51869	0.54655	0.55382	0.73511	0.51869
	1.5	0.83734	1.03988	1.31022	0.62897	0.67024	0.68111	0.90147	0.62897
	2.0	0.88128	1.10739	1.41398	0.67938	0.72770	0.74048	0.97875	0.67938
	3.0	0.92188	1.17112	1.51401	0.72412	0.77918	0.79381	1.04801	0.72412
	5.0	0.94856	1.21371	1.58198	0.75227	0.81181	0.82766	1.09188	0.75227
3	0.5	0.30440	0.32879	0.35581	-0.02616	-0.02610	-0.02608	-0.03510	-0.02616
	1.0	0.56428	0.65193	0.75818	0.33637	0.34794	0.35092	0.46798	0.33637
	1.5	0.65502	0.77502	0.92519	0.44664	0.46720	0.47253	0.62839	0.44664
	2.0	0.69895	0.83665	1.01165	0.49706	0.52260	0.52926	0.70290	0.49706
	3.0	0.73956	0.89483	1.09500	0.54180	0.57225	0.58021	0.76967	0.54180
	5.0	0.76624	0.93370	1.15165	0.56995	0.60370	0.61255	0.81198	0.56995
5	0.5	-0.20643	-0.19613	-0.18651	-0.23675	-0.53699	-0.50916	-0.50251	-0.68482
	1.0	0.05345	0.05417	0.05491	0.06539	-0.17446	-0.17145	-0.17071	-0.23060
	1.5	0.14420	0.14952	0.15511	0.18049	-0.06418	-0.06377	-0.06367	-0.08577
	2.0	0.18813	0.19726	0.20699	0.23811	-0.01377	-0.01375	-0.01375	-0.01850
	3.0	0.22873	0.24232	0.25700	0.29251	0.03098	0.03107	0.03110	0.04179
	5.0	0.25541	0.27244	0.29099	0.32886	0.05912	0.05947	0.05956	0.07999

Table 4. Numerical values of the entropy for the TIIHLA distribution ($\vartheta = 1.5$or $\vartheta = 2$)

$\psi \uparrow$	$\delta \uparrow$	$\vartheta = 1.5$				$\vartheta = 2$			
		$RE(\vartheta) \uparrow$	$TE(\vartheta) \uparrow$	$AE(\vartheta) \uparrow$	$HCE(\vartheta) \uparrow$	$RE(\vartheta) \uparrow$	$TE(\vartheta) \uparrow$	$AE(\vartheta) \uparrow$	$HCE(\vartheta) \uparrow$
0.5	0.5	1.36591	0.98975	1.09723	1.68962	1.20724	0.70098	0.90634	1.40196
	1.0	1.88280	1.21984	1.39838	2.08239	1.79273	0.83350	1.18390	1.66699
	1.5	2.01490	1.26970	1.46738	2.16751	1.93247	0.85521	1.23897	1.71042
	2.0	2.07214	1.29031	1.49634	2.20269	1.99206	0.86359	1.26131	1.72717
	3.0	2.12131	1.30754	1.52079	2.23211	2.04278	0.87033	1.27981	1.74067
	5.0	2.15127	1.31784	1.53549	2.24969	2.07344	0.87425	1.29077	1.74850
1	0.5	0.67276	0.57130	0.60266	0.97526	0.51409	0.40196	0.45333	0.80391
	1.0	1.18965	0.89668	0.98209	1.53073	1.09959	0.66699	0.84586	1.33398
	1.5	1.32175	0.96720	1.06902	1.65111	1.23932	0.71042	0.92375	1.42084
	2.0	1.37899	0.99634	1.10551	1.70086	1.29891	0.72717	0.95534	1.45434
	3.0	1.42816	1.02072	1.13631	1.74247	1.34964	0.74067	0.98150	1.48133
	5.0	1.45812	1.03528	1.15483	1.76733	1.38030	0.74850	0.99700	1.49699
2	0.5	-0.02039	-0.02049	-0.02046	-0.03498	-0.17906	-0.19609	-0.18732	-0.39218
	1.0	0.49650	0.43967	0.45759	0.75057	0.40644	0.33398	0.36780	0.66796
	1.5	0.62860	0.53940	0.56711	0.92082	0.54617	0.42084	0.47795	0.84168
	2.0	0.68585	0.58061	0.61310	0.99117	0.60576	0.45434	0.52263	0.90868
	3.0	0.73502	0.61509	0.65190	1.05002	0.65649	0.48133	0.55963	0.96266
	5.0	0.76497	0.63567	0.67523	1.08516	0.68715	0.49699	0.58154	0.99398
2.5	0.5	-0.24353	-0.25898	-0.25369	-0.40220	-0.49511	-0.44550	-0.99023	-0.40220
	1.0	0.27336	0.25550	0.26127	0.18330	0.16748	0.17515	0.33496	0.18330
	1.5	0.40546	0.36700	0.37925	0.32303	0.27605	0.29829	0.55210	0.32303
	2.0	0.46270	0.41308	0.42879	0.38262	0.31793	0.34825	0.63585	0.38262
	3.0	0.51187	0.45162	0.47059	0.43334	0.35166	0.38961	0.70333	0.43334
	5.0	0.54183	0.47464	0.49572	0.46401	0.37124	0.41411	0.74248	0.46401
3	0.5	-0.42585	-0.47459	-0.45756	-0.81017	-0.58452	-0.79414	-0.67891	-1.58827
	1.0	0.09104	0.08900	0.08967	0.15192	0.00097	0.00097	0.00097	0.00195
	1.5	0.22314	0.21114	0.21504	0.36044	0.14071	0.13126	0.13587	0.26251
	2.0	0.28038	0.26161	0.26768	0.44660	0.20030	0.18151	0.19059	0.36302
	3.0	0.32955	0.30383	0.31210	0.51867	0.25102	0.22200	0.23591	0.44399
	5.0	0.35951	0.32905	0.33880	0.56172	0.28168	0.24549	0.26275	0.49098
5	0.5	-0.93668	-1.19468	-1.09939	-2.03944	-1.09535	-1.99022	-1.45845	-3.98045
	1.0	-0.41979	-0.46710	-0.45058	-0.79738	-0.50985	-0.66505	-0.58073	-1.33009
	1.5	-0.28769	-0.30941	-0.30194	-0.52820	-0.37012	-0.44791	-0.40658	-0.89581
	2.0	-0.23045	-0.24425	-0.23953	-0.41696	-0.31053	-0.36415	-0.33594	-0.72830
	3.0	-0.18127	-0.18974	-0.18686	-0.32391	-0.25980	-0.29667	-0.27743	-0.59335
	5.0	-0.15132	-0.15719	-0.15520	-0.26834	-0.22914	-0.25752	-0.24278	-0.51504

where,

$$\eta^*_{i,j,v,b,l}=2^{i+j}\,(-1)^{v+b+i+j}\,(i+1)\binom{(i+1)\delta-1}{j}\binom{j}{k}\binom{n-i}{j}\binom{i+j+v-2}{v}\binom{\delta(v+i+j-1)}{b}\binom{b}{l}\delta\,\psi^{k+l+2},$$

and $Beta(a,b)=\int_0^1 s^{a-1}(1-s)^{b-1}ds$ refers to the beta function.

7. Parameters Estimation

ML estimation represents a principal method for determining distribution parameters. This technique involves maximizing the likelihood function to determine the parameter values under which the observed data are most likely, given a specific statistical model. As a result of its efficacy, the ML method finds broad application in disciplines such as economics, finance, and the biological sciences for parameter inference and predictive analysis.

This section explores the ML estimators for the parameters of the proposed model. Let $w_1,\ w_2,\ \ldots,\ w_n$ be a random sample of size n drawn from the TIIHLA distribution; parameterized by ψ and δ. Define $\Upsilon = (\psi,\quad \delta)^T$ as the parameters vector, the *log-likelihood function* (LL) for the TIIHLA model is expressed as:

$$\Delta_n = n\log[2\,\delta] + 2n\log[\psi] + \sum_{i=1}^{n}\log[w_i] + (\delta-1)\sum_{i=1}^{n}\log\left[1-(1+\psi\ w_i)\ \mathrm{e}^{-\psi w_i}\right]$$

$$-2\sum_{i=1}^{n}\log\left[1+\left(1-(1+\psi w_i)\ \mathrm{e}^{-\psi w_i}\right)^{\delta}\right] - \psi\sum_{i=1}^{n} w_i\ . \tag{7.1}$$

The ML equations are obtained by differentiating Equation (7.1) with respect to parameters ψ and δ. The resulting equations are given, respectively, by:

$$\frac{\partial\Delta_n}{\partial\hat{\psi}} = \frac{2n}{\hat{\psi}} - \sum_{i=1}^{n} w_i - (\hat{\delta}-1)\sum_{i=1}^{n}\frac{w_i\,\mathrm{e}^{-\hat{\psi}\,w_i} - w_i\,(1+\hat{\psi}\ w_i)\,\mathrm{e}^{-\hat{\psi}\,w_i}}{1-(1+\hat{\psi}\ w_i)\,\mathrm{e}^{-\hat{\psi}\,w_i}}$$

$$-2\sum_{i=1}^{n}\frac{\hat{\delta}\,\hat{\psi}\,{w_i}^2\left[1-(1+\hat{\psi}\ w_i)\,\mathrm{e}^{-\hat{\psi}\,w_i}\right]^{\hat{\delta}-1}\ \mathrm{e}^{-\hat{\psi}\,w_i}}{1+\left[1-(1+\hat{\psi}\ w_i)\,\mathrm{e}^{-\hat{\psi}\,w_i}\right]^{\hat{\delta}}} = 0\ , \tag{7.2}$$

and

$$\frac{\partial\Delta_n}{\partial\hat{\delta}} = \frac{n}{\hat{\delta}} + \sum_{i=1}^{n}\log\left[1-(1+\hat{\psi}\ w_i)\ \mathrm{e}^{-\hat{\psi}\,w_i}\right]$$

$$-2\sum_{i=1}^{n}\frac{\log\left[1-(1+\hat{\psi}\ w_i)\ \mathrm{e}^{-\hat{\psi}\,w_i}\right]\left(1-(1+\hat{\psi}\ w_i)\ \mathrm{e}^{-\hat{\psi}\,w_i}\right)^{\hat{\delta}}}{1+\left(1-\left[(1+\hat{\psi}\ w_i)\right]\mathrm{e}^{-\hat{\psi}\,w_i}\right)^{\hat{\delta}}} = 0\ . \tag{7.3}$$

Newton's method, or other optimization algorithms, can be employed to solve Equations ((7.2)–(7.3)) by identifying the parameter vector $\widehat{\Upsilon}=\left(\hat{\psi},\quad\hat{\delta}\right)^T$ that maximizes the likelihood function, thus evaluating model fit.

8. Simulation Study

Monte Carlo simulation approximates the desired parameters through iterative random sampling of input values, subsequent execution of simulations based on these values, and rigorous analysis of the resultant data. This approach proves particularly beneficial for estimating complex models where analytical solutions are either impractical or infeasible. This simulation technique is commonly utilized in various areas, including finance, engineering, and physics. It can be used to estimate the probability distribution of the outcomes and verify a model's response to different input parameters. In this study, we performed 1000 iterations of the simulation, with Equation (2.1) generating sample sizes of (50, 100, 150, 200, 300, 400 and 500), to evaluate the efficiency of the TIIHLA model through its parameter vector $\Upsilon = (\psi, \delta)$. The actual parameter values for the simulated estimates were: Case I: ($\psi = 2$, $\delta = 0.5$), Case II: ($\psi = 3$, $\delta = 1$), Case III: ($\psi = 5$, $\delta = 4$)and Case IV: ($\psi = 10$, $\delta = 7.5$).
The parameters were estimated by optimizing the LL presented in Equation (7.1) using the Newton-Raphson method in Wolfram Mathematica 13. A ML estimation method was employed. To evaluate the accuracy of the ML estimates at a 95% confidence level, we computed the average parameter estimates, *mean squared errors* (MSE), *average bias* (Bias), *coverage probability* (CP) and the *average length of the confidence intervals* (CI). The following equations were used to obtain the average MSEs and bias from the simulated estimates:
$MSE_{\Upsilon}(n) = \frac{1}{1000}\sum_{i=1}^{1000}\left(\widehat{\Upsilon}_i - \Upsilon\right)^2$ and $Bias_{\Upsilon}(n) = \frac{1}{1000}\sum_{i=1}^{1000}\left(\widehat{\Upsilon}_i - \Upsilon\right)$ where, $\Upsilon = (\psi, \quad \delta)$.
The CP measures the reliability of confidence intervals by quantifying the proportion of times they contain the true parameter value across repeated samples or simulations. A CP close to the nominal confidence level (e.g., 95%) indicates accurate interval estimation by the estimation method.
Tables 5-8 reveal that, as n increases, the ML estimates reach the optimal dimensions for all parameter choices. As n increases, the MSEs decrease until they reach zero, as expected. Furthermore, the CPs of the confidence intervals roughly match the assumed certainty level (95%). With a larger sample size, the CI for each parameter increases, indicating that asymptotic results are effective at estimating and describing confidence intervals.

Table 5. Numerical outcomes [Case – I]

$\psi = 2$	$n = 50$	$n = 100$	$n = 150$	$n = 200$	$n = 300$	$n = 400$	$n = 500$
$\hat{\psi}$	2.135910	2.077140	2.060160	2.049040	2.040000	2.033080	2.032750
$Bias$	0.135910	0.077141	0.060164	0.049044	0.040003	0.033077	0.032749
MSE	0.227135	0.107547	0.066695	0.049518	0.032577	0.022901	0.019175
95% CI	1.791540	1.250090	0.984996	0.851283	0.690276	0.579161	0.527675
95 % CP	0.932	0.938	0.936	0.936	0.94	0.943	0.947
$\delta = 0.5$	$n = 50$	$n = 100$	$n = 150$	$n = 200$	$n = 300$	$n = 400$	$n = 500$
$\hat{\delta}$	0.530308	0.518168	0.514730	0.512799	0.511442	0.510041	0.509683
$Bias$	0.030308	0.018168	0.014730	0.012799	0.011442	0.010041	0.009684
MSE	0.007856	0.003412	0.002196	0.001671	0.001153	0.000831	0.000707
95% CI	0.326671	0.217724	0.174463	0.152272	0.125377	0.105975	0.097141
95 % CP	0.929	0.934	0.933	0.931	0.931	0.934	0.934

Table 6. Numerical outcomes [Case – II]

$\psi = 3$	$n = 50$	$n = 100$	$n = 150$	$n = 200$	$n = 300$	$n = 400$	$n = 500$
$\hat{\psi}$	3.120690	3.057490	3.040640	3.029160	3.019420	3.012370	3.011960
$Bias$	0.120690	0.057485	0.040641	0.029165	0.019424	0.012369	0.011962
MSE	0.306628	0.148985	0.0910388	0.0687088	0.0452946	0.0323819	0.0266562
95% CI	2.119540	1.496940	1.172580	1.021660	0.831209	0.704087	0.638607
95 % CP	0.939	0.948	0.94	0.946	0.947	0.949	0.95
$\delta = 1$	$n = 50$	$n = 100$	$n = 150$	$n = 200$	$n = 300$	$n = 400$	$n = 500$
$\hat{\delta}$	1.057890	1.026410	1.017910	1.013150	1.009430	1.006110	1.005240
$Bias$	0.057892	0.026408	0.017908	0.013153	0.009428	0.006113	0.005241
MSE	0.044585	0.018555	0.011530	0.008671	0.005783	0.004110	0.003451
95% CI	0.796391	0.524100	0.415226	0.361537	0.295958	0.250290	0.229464
95 % CP	0.929	0.934	0.933	0.931	0.931	0.934	0.934

Table 7. Numerical outcomes [Case – III]

$\psi = 5$	$n = 50$	$n = 100$	$n = 150$	$n = 200$	$n = 300$	$n = 400$	$n = 500$
$\hat{\psi}$	5.135670	5.062630	5.044420	5.028930	5.020140	5.01267	5.012060
$Bias$	0.135670	0.062633	0.044423	0.028926	0.020143	0.0126666	0.012061
MSE	0.474832	0.234677	0.141511	0.0851737	0.071571	0.0521852	0.0422785
95% CI	2.649650	1.883990	1.465040	1.138970	1.046250	0.894557	0.805035
95 % CP	0.941	0.949	0.951	0.942	0.946	0.952	0.949
$\delta = 4$	$n = 50$	$n = 100$	$n = 150$	$n = 200$	$n = 300$	$n = 400$	$n = 500$
$\hat{\delta}$	4.399700	4.179020	4.118290	4.074970	4.058830	4.038730	4.033120
$Bias$	0.399703	0.179024	0.118285	0.074968	0.058827	0.038732	0.033122
MSE	1.792740	0.681520	0.393892	0.228786	0.190824	0.135055	0.112102
95% CI	5.011790	3.160700	2.417340	1.852750	1.697640	0.948000	1.306700
95 % CP	0.939	0.947	0.938	0.942	0.954	0.946	0.941

Table 8. Numerical outcomes [Case – IV]

$\psi = 10$	$n = 50$	$n = 100$	$n = 150$	$n = 200$	$n = 300$	$n = 400$	$n = 500$
$\hat{\psi}$	10.25150	10.1157	10.0822	10.0589	10.0373	10.0238	10.022500
$Bias$	0.251472	0.11565	0.08215	0.05893	0.03726	0.02383	0.022482
MSE	1.640050	0.81019	0.48613	0.37119	0.24648	0.18058	0.145615
95% CI	4.924850	3.50092	2.71545	2.37825	1.94164	1.66402	1.494000
95 % CP	0.942	0.949	0.951	0.95	0.947	0.949	0.95
$\delta = 7.5$	$n = 50$	$n = 100$	$n = 150$	$n = 200$	$n = 300$	$n = 400$	$n = 500$
$\hat{\delta}$	8.48006	7.93606	7.78470	7.70982	7.64058	7.59426	7.580530
$Bias$	0.98006	0.43606	0.28470	0.20982	0.14058	0.09426	0.080529
MSE	10.00220	3.57563	1.98689	1.47034	0.94561	0.66643	0.550020
95% CI	11.79310	7.21629	5.41435	4.68393	3.77375	3.18027	2.891460
95 % CP	0.940	0.944	0.937	0.944	0.951	0.945	0.943

9. Applications

Several publications have used AD to look at data for a component reliability investigation. This study employed two real data sets to demonstrate the adaptability of the TIIHLA model in the field of medical science. The first data set includes COVID-19 mortality rates in the United Kingdom over a 76-day period, from April 15 to June 30, 2020. Mubarak and Almetwally [31] recently investigated this data. The second dataset, established by [32], has 128 records demonstrating the durations of radiation therapy (measured in months) of people who were diagnosed with bladder cancer.

In each case, the ML approach was used to estimate the distribution parameters. The versatility of the proposed model was evaluated using several criteria: the *negative log-likelihood* (-LL), *Akaike's information criterion* (AIC), *Bayesian information criterion* (BIC) and *Hannan-Quinn information criterion* (HQIC). In addition, supplemental performance measures, including: the *Anderson-Darling* (A^*), Cramér-Von Mises (W^*) and *Kolmogorov-Smirnov statistic* (K-S) *along with P-value*; were applied to help identify the most suitable model among the alternatives. Ultimately, the model that recorded the lowest scores along with the highest *P*-value for the K-S test was considered the most effective.

We examined the precision of the TIIHLA distribution to five alternative lifetime models, which are presented in the table below.

Table 9. The competitive lifetime models

Distribution	Abbreviation	CDF	Authors
Ailamujia	AD	$F_w(\psi) = 1 - (1 + \psi\, w)\, e^{-\psi w}\ ;\ w > 0,\ \psi > 0$	[1]
Exponentiated Ailamujia	EA	$F_w(\psi, \gamma) = \left[1 - (1 + 2\psi\ w)\, e^{-2\psi x}\right]^{\gamma}\ ;\ w > 0, \psi > 0, \gamma > 0$	[7]
Exponentiated Exponential	EE	$F_w(\psi, \lambda) = \left[1 - e^{-\psi w}\right]^{\lambda}\ ;\ w > 0, \psi > 0,\ \lambda > 0$	[33]
Gamma	GD	$F_w(\psi, \alpha) = \frac{\Gamma(\alpha, \psi\, w)}{\Gamma(\alpha)}\ ;\ w > 0, \psi > 0, \alpha > 0$	[34]
Generalized Lindley	GL	$F_w(\psi, \theta) = \left[1 - \frac{(1+\psi+\psi\, w)e^{-\psi w}}{1+\psi}\right]^{\theta};\ w > 0, \psi > 0, \theta > 0$	[35]

Ref. [36] developed a *total time test* (TTT) plot, a powerful graphical tool for evaluating the suitability of data for a specified distribution. Figure 6 illustrates the TTT plots for both datasets. As noted in Aarset's study, the TTT plot for the COVID-19 data exhibits a convex shape, which indicates that its empirical hazard rate is decreasing. In contrast, the TTT plot for bladder cancer diagnostic data displays a concave-convex pattern that resembles an upside-down bathtub shape in its hazard rate.

Tables 10 and 13 present the ML estimates for the parameters of each competitive model for the respective datasets, with *standard errors* (SEs) provided in parentheses. Simultaneously, Figures 7 and 10 illustrate the profile log-likelihood functions for various parameter values within the ML framework. These functions exhibit a distinctly concave shape with clear peaks corresponding to the ML estimates, thereby confirming a unique solution for parameter estimation.

Tables 11 and 12 display the goodness of fit measures for COVID-19 data, including (-LL, AIC, BIC and HQIC) along with the empirical results for the (A^*, W^*, K-S and *P*-value (K-S)). Similarly, Tables 14 and 15 provide comparable metrics for bladder cancer data.

Figures 8 and 11 display the estimated pdf and the estimated SF for both data sets, while Figures 9 and 12 provide the Q–Q plots for all fitted models. These visual representations of Covid-19 and bladder cancer data align with the numerical findings, clearly highlighting the superior fit of the proposed model compared to the alternative distributions.

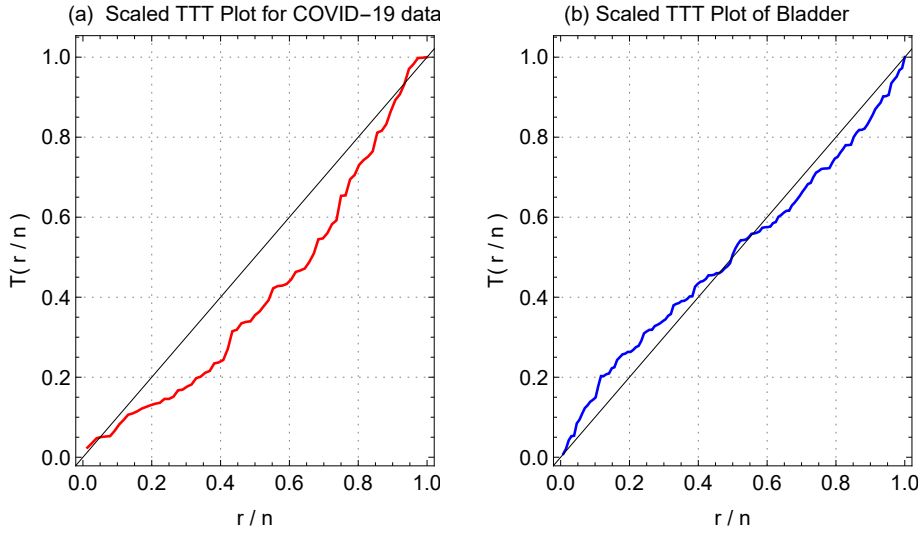

Figure 6. TTT Plots for (a) COVID-19 data and (b) bladder cancer data.

Table 10. The ML estimates and their SEs are in parentheses for the COVID-19 data

Model	Estimates	
TIIHLA(ψ, δ)	$\hat{\psi} = 0.381825$	$\hat{\delta} = 0.48179$
	(0.065261)	(0.059488)
EA(ψ, γ)	$\hat{\psi} = 0.227915$	$\hat{\gamma} = 0.383405$
	(0.034752)	(0.054577)
EE(ψ, λ)	$\hat{\psi} = 0.353033$	$\hat{\lambda} = 0.800936$
	(0.056935)	(0.117064)
GL(ψ, θ)	$\hat{\psi} = 0.617324$	$\hat{\theta} = 0.49989$
	(0.092947)	(0.067401)
GD(ψ, α)	$\hat{\psi} = 0.803738$	$\hat{\alpha} = 3.03233$
	(0.112543)	(0.575166)
AD(ψ)	$\hat{\psi} = 0.820616$	-
	(0.066561)	-

Table 11. -LL, AIC, BIC and HQIC statistics for the COVID-19 data

Model	-LL	AIC	BIC	HQIC
TIIHLA	140.6870	285.3750	290.0360	287.2380
EA	142.8640	289.7280	294.3890	291.5910
EE	142.5030	289.0060	293.6670	290.8690
GL	145.3660	294.7310	299.3930	296.5940
GD	142.4100	288.8210	293.4820	290.6840
AD	170.4310	342.8620	345.1930	343.7940

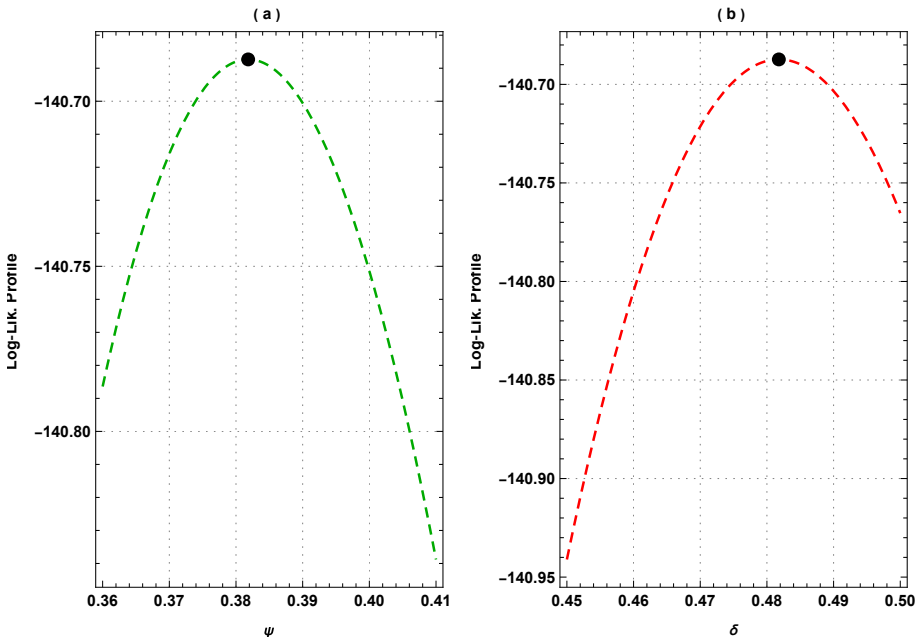

Figure 7. Plots of the log-likelihood profile for COVID-19 data.

Table 12. The A*, W*, K-S and *P*-value (K-S) metrics for the COVID-19 data

Model	A*	W*	K-S	*P*-Value (K-S)
TIIHLA	0.638491	0.095125	0.081957	0.687002
EA	1.152040	0.196822	0.100622	0.424959
EE	1.038420	0.173011	0.098546	0.451593
GL	1.595560	0.271653	0.111173	0.304503
GD	0.984292	0.161130	0.096156	0.483318
AD	16.794600	1.946630	0.282402	1.09E-05

10. Concluding Remarks

This paper describes a novel two-parameter distribution constructed from the type II half-logistic-G family and Ailamujia distribution. This distribution is referred to as the type II half-logistic Ailamujia distribution. A number of statistical characteristics were computed for the type II half-logistic Ailamujia distribution. These characteristics include moments, moment-generating function, probability-weighted moment, incomplete moments, conditional moments, mean deviation, Lorenz and Bonferroni curves, mean residual life, mean inactivity time, and order statistics. Calculations and theoretical and numerical discussions were conducted using several uncertainty metrics. In addition, the maximum likelihood estimation technique is utilized to estimate the two parameters of the type II half-logistic Ailamujia distribution. A comprehensive numerical procedure was performed to determine whether the maximum likelihood estimation technique was effective. Examining two real

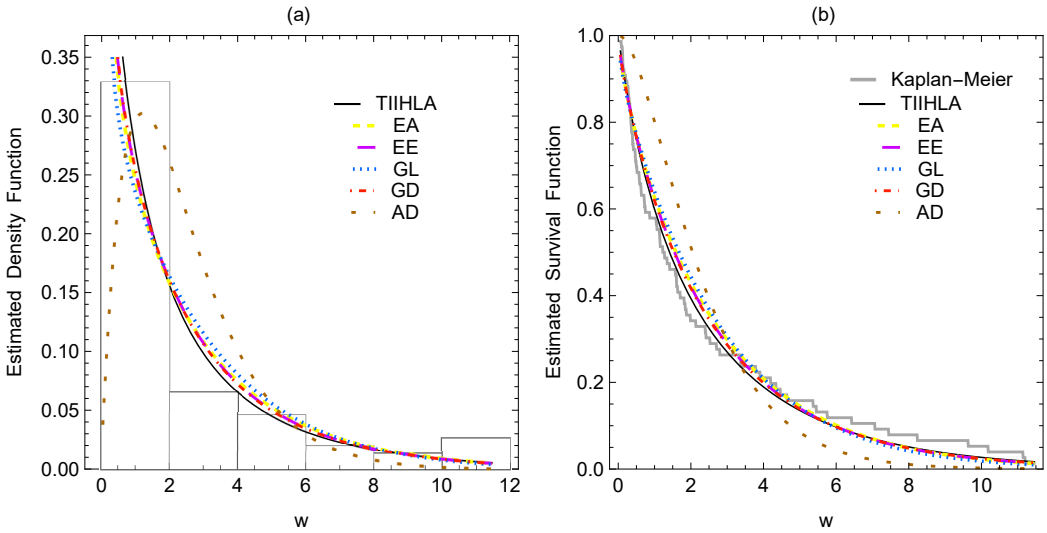

Figure 8. Plots of the (a) estimated pdf and (b) estimated SF for COVID-19 data.

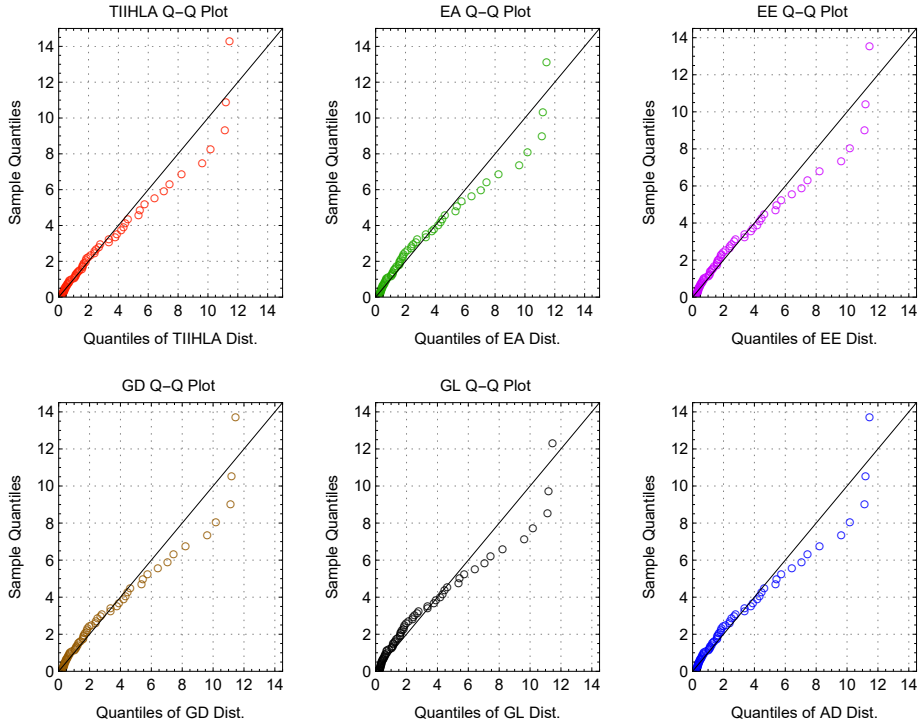

Figure 9. Q-Q plots for the COVID-19 data

Table 13. The ML estimates and their SEs (in parentheses) for the bladder cancer data

Model	Estimates	
TIIHLA(ψ, δ)	$\hat{\psi} = 0.127061$	$\hat{\delta} = 0.696652$
	(0.015033)	(0.072639)
EA(ψ, γ)	$\hat{\psi} = 0.077055$	$\hat{\gamma} = 0.570522$
	(0.008243)	(0.067672)
EE(ψ, λ)	$\hat{\psi} = 0.121167$	$\hat{\lambda} = 1.21795$
	(0.013573)	(0.148836)
GL(ψ, θ)	$\hat{\psi} = 0.733631$	$\hat{\theta} = 0.16487$
	(0.09117)	(0.016635)
GD(ψ, α)	$\hat{\psi} = 1.17251$	$\hat{\alpha} = 7.98766$
	(0.130835)	(1.10433)
AD(ψ)	$\hat{\psi} = 0.213547$	-
	(0.013347)	-

Table 14. -LL, AIC, BIC and HQIC statistics for bladder cancer data

Model	-LL	AIC	BIC	HQIC
TIIHLA	411.7190	827.4390	833.1430	829.7560
EA	414.5260	833.0520	838.7560	835.3690
EE	413.0780	830.1550	835.8590	832.4730
GL	416.2860	836.5720	842.2760	838.8890
GD	413.3680	830.7360	836.4400	833.0530
AD	426.7970	855.5930	858.4450	856.7520

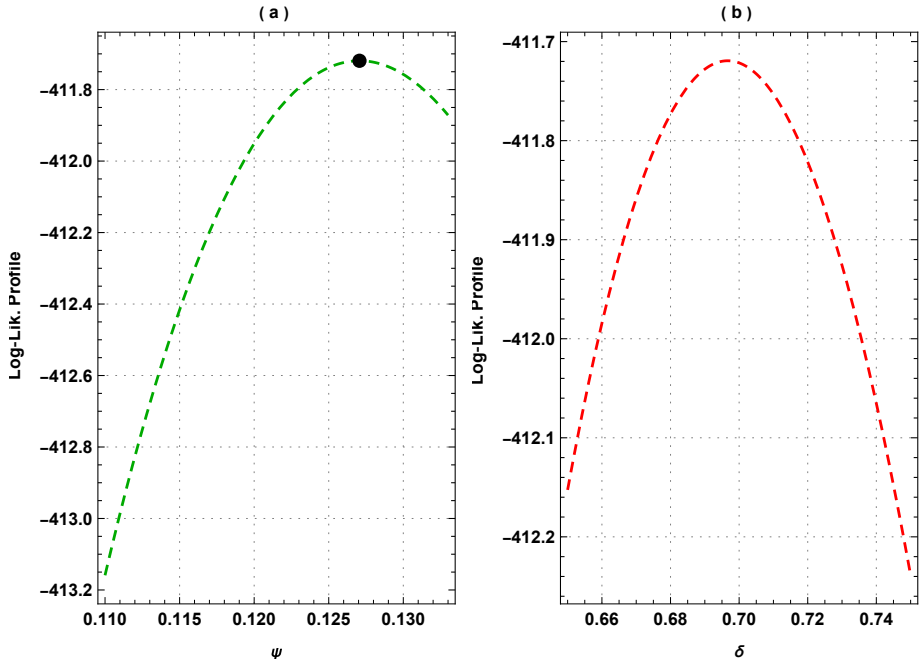

Figure 10. Plots of the log-likelihood profile for bladder cancer data.

Table 15. The A*, W*, K-S and *P*-value (K-S) metrics for the bladder cancer data

Model	A*	W*	K-S	*P*-value (K-S)
TIIHLA	0.467076	0.080071	0.059393	0.757272
EA	1.015740	0.187000	0.083640	0.332073
EE	0.718193	0.128403	0.072515	0.511320
GL	1.332020	0.247859	0.092790	0.220388
GD	0.776249	0.136063	0.073295	0.497389
AD	5.391120	0.841091	0.141385	0.011984

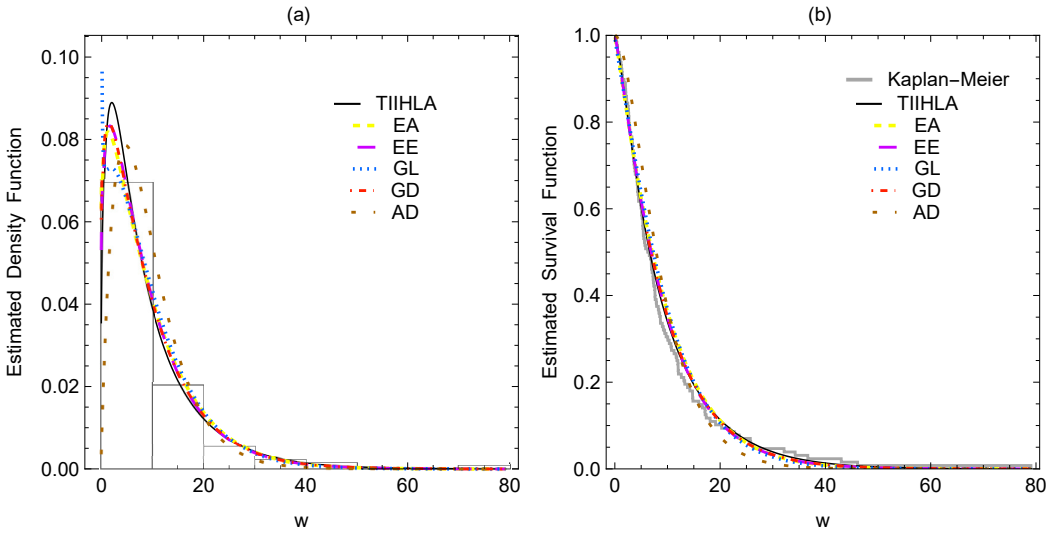

Figure 11. Plots of the (a) estimated pdf and (b) estimated SF for the bladder cancer data.

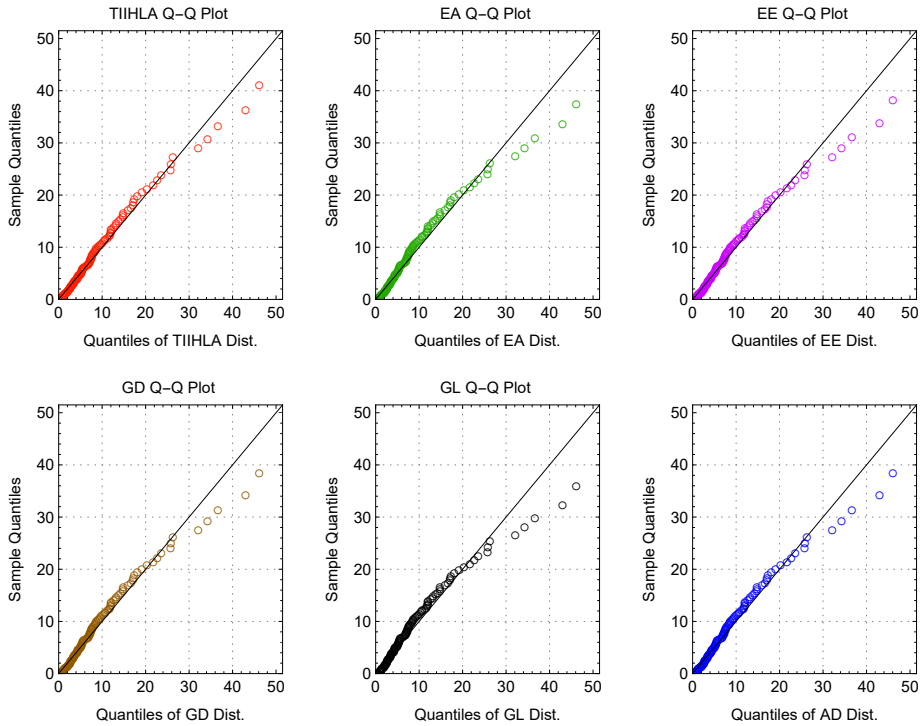

Figure 12. Q-Q plots for the bladder cancer data

datasets makes it possible to determine the applicability and importance of the recently developed model. Several well-known statistical distributions, including the Ailamujia, exponentiated Ailamujia, exponentiated exponential, gamma, and generalized Lindley models, are compared to the type II half-logistic Ailamujia distribution. This comparison was performed using a variety of metrics. According to the results of the numerical analysis, the type II half-logistic Ailamujia model provided the best fit for the data compared to the other competing models. The limitation of this article lies in the estimation of the distribution parameters using the maximum likelihood estimation technique only using the complete samples. Therefore, in the future, we intend to use Bayesian and other estimate techniques for parameter estimation of the type II half-logistic Ailamujia model utilizing different censoring schemes.

Data Availability: The data that support the findings of this study are available upon request from the corresponding author.

Author contributions: All authors have accepted responsibility for the entire content of this manuscript and approved its submission.

Conflicts of Interest: The authors declare no conflicts of interest.

References

1. Lv, H. Q., Gao, L. H., & Chen, C. L. (2002). Ailamujia distribution and its application in supportability data analysis. Journal of Academy of Armored Force Engineering, 16(3), 48–52.
2. Pan, G. T., Wang, B. H., Chen, C. L., Huang, Y. B., & Dang, M. T. (2009). The research of interval estimation and hypothetical test of small sample of distribution. Application of Statistics and Management, 28, 468–472.
3. Bing, L. O. N. G. (2015). Bayesian estimation of parameter on 3-parameter distribution under different prior distributions. Mathematics in Practice and Theory.
4. Yu, C. M., Chi, Y. H., Zhao, Z. W., & Song, J. F. (2015). Maintenance-decision-oriented modeling and emulating of battlefield injury in campaign macrocosm. Journal of System Simulation, 20, 5669–5671.
5. Jan, U., Fatima, K., & Ahmad, S. P. (2017). On weighted Ailamujia distribution and its applications to lifetime data. Journal of Statistics Applications and Probability, 6, 619–633.
6. Jamal, F., Chesneau, C., Aidi, K., & Ali, A. (2021). Theory and application of the power Ailamujia distribution. Journal of Mathematical Modeling, 9, 391–413.
7. Rather, A. A., Subramanian, C., Al-Omari, A. I., & Alanzi, A. R. A. (2022). Exponentiated Ailamujia distribution with statistical inference and applications of medical data. Journal of Statistics and Management Systems. https://doi.org/10.1080/09720510.2021.1966206
8. Gomaa, R. S., Hebeshy, E. A., El Genidy, M. M., & El-Desouky, B. S. (2023). Alpha-power of the power Ailamujia distribution: Properties and applications. Journal of Statistics Applications & Probability, 12(2), 701–723.
9. Al-nefaie, A. H., & Ragab, I. E. (2022). A novel lifetime model with a bathtub-shaped hazard rate: Properties and applications. Journal of Applied Science and Engineering, 26(3), 413–421.

10. Jan, R., Jan, T. R., Ahmad, P. B., & Bashir, R. (2020). A new generalization of Ailamujia distribution with real-life applications. 2020 8th International Conference on Reliability, Infocom Technologies and Optimization (Trends and Future Directions) (ICRITO), 237–242. https://doi.org/10.1109/ICRITO48877.2020.9197844
11. Ahmad, A., ul Ain, S. Q., Ahmad, A., & Tripathi, R. (2022). The weighted inverse Ailamujia distribution with applications to real-life data. Pakistan Journal of Statistics, 38(4), 451–471.
12. Tahir, M. H., Cordeiro, G. M., Alzaatreh, A., Mansoor, M., & Zubair, M. (2016). The logistic-X family of distributions and its applications. Communications in Statistics-Theory and Methods, 45(24), 7326–7349.
13. Zografos, K., & Balakrishnan, N. (2009). On families of beta- and generalized gamma-generated distributions and associated inference. Statistical Methodology, 6, 344–362.
14. Kumar, D., Singh, U., & Singh, S. K. (2015). A new distribution using sine function: Its application to bladder cancer patients' data. Journal of Statistics Applications & Probability, 4(3), 417–427.
15. Cordeiro, G. M., & de Castro, M. (2011). A new family of generalized distributions. Journal of Statistical Computation and Simulation, 81, 883–898.
16. Ahmad, A., Mahmoudi, E., & Dey, S. (2020). A new family of heavy-tailed distributions with an application to heavy-tailed insurance loss data. Communications in Statistics-Simulation and Computation, 51(8), 4372–4395.
17. Alexander, C., Cordeiro, G. M., Ortega, E. M. M., & Sarabia, J. M. (2012). Generalized beta-generated distributions. Computational Statistics & Data Analysis, 56, 1880–1897.
18. Abdelall, Y. Y., Hassan, A. S., & Almetwally, E. M. (2024). A new extention of the odd inverse Weibull-G family of distributions: Bayesian and non-Bayesian estimation with engineering applications. Computational Journal of Mathematical and Statistical Sciences, 3(2), 359-388.
19. Kharazmi, O., Saadatinik, A., Alizadeh, M., & Hamedani, G. G. (2019). Odd hyperbolic cosine-FG family of lifetime distributions. Journal of Statistical Theory and Applications, 18, 387–401.
20. Nadarajah, S., Cordeiro, G. M., & Ortega, E. M. M. (2015). The Zografos–Balakrishnan-G family of distributions: Mathematical properties and applications. Communications in Statistics-Theory and Methods, 44, 186–215.
21. Ahmad, W., Afify, Z., & Goual, H. (2020). The arcsine exponentiated-X family: Validation and insurance application. Complexity, 2020, Article ID 8394815.
22. Almarashi, M., Jamal, F., Chesneau, C., & Elgarhy, M. (2021). A new truncated Muth-generated family of distributions with applications. Complexity, 2021, Article ID 1211526.
23. Al-Moisheer, A. S., Elbatal, I., Almutiry, W., & Elgarhy, M. (2021). Odd inverse power generalized Weibull generated family of distributions: Properties and applications. Mathematical Problems in Engineering, 2021, Article ID 5082192.
24. Hassan, A. S., Elgarhy, M., & Shakil, M. (2017). Type II half-logistic family of distributions with applications. Pakistan Journal of Statistics & Operations Research, 13(2), 245–264.
25. Greenwood, J. A., Landwehr, J. M., Matalas, N. C., & Wallis, J. R. (1979). Probability-weighted moments: Definition and relation to parameters of several distributions expressible in inverse form. Water Resources Research, 15(5), 1049–1054.

26. Renner, R., & Wolf, S. (2004). Smooth Rényi entropy and applications. In Proceedings of the International Symposium on Information Theory (p. 233). IEEE.

27. Shannon, C. E. (1948). A mathematical theory of communication. The Bell System Technical Journal, 27(3), 379–423.

28. Tsallis, C. (2019). Beyond Boltzmann–Gibbs–Shannon in physics and elsewhere. Entropy, 21(7), p.696.

29. Arimoto, S. (1971). Information-theoretical considerations on estimation problems. Information and Control, 19(3), 181–194.

30. Havrda, J., & Charvát, F. (1967). Quantification method of classification processes: Concept of structural a-entropy. Kybernetika, 3(1), 30–35.

31. Mubarak, A. E., & Almetwally, E. M. (2021). A new extension exponential distribution with applications of COVID-19 data. Journal of Financial and Business Research, 22(1), 444–460.

32. Wang, X., Lee, S. R., Arai, K., Tsuji, K., Rebeck, G. W., & Lo, E. H. (2003). Lipoprotein receptor-mediated induction of matrix metalloproteinase by tissue plasminogen activator. Nature Medicine, 9(10), 1313–1317.

33. Gupta, R. D., & Kundu, D. (2001). Exponentiated exponential family: An alternative to gamma and Weibull distributions. Biometrical Journal: Journal of Mathematical Methods in Biosciences, 43(1), 117–130.

34. Johnson, N. L., Kotz, S., & Balakrishnan, N. (1995). Continuous univariate distributions, Volume 2. New York: John Wiley & Sons.

35. Nadarajah, S., Bakouch, H. S., & Tahmasbi, R. (2011). A generalized Lindley distribution. Sankhya B, 73, 331–359.

36. Aarset, M. V. (1987). How to identify a bathtub hazard rate. IEEE Transactions on Reliability, 36(1), 106–108.